



Cite this: *Polym. Chem.*, 2024, **15**, 1227

# Ring-opening polymerisation of alkyl-substituted $\epsilon$ -caprolactones: kinetic effects of substitution position†

Cinzia Clamor,<sup>a</sup> James Beament,<sup>b</sup> Peter M. Wright,<sup>b</sup> Beatrice N. Cattoz,<sup>b</sup> Rachel K. O'Reilly <sup>\*a</sup> and Andrew P. Dove <sup>\*a</sup>

Ring-opening polymerisation (ROP) of lactones has been proven as a powerful technique to generate polyesters with high levels of control over molar mass and polymer dispersity. However, the introduction of functional groups on the monomer ring structure can dramatically influence the ability of a monomer to undergo ROP. Therefore, understanding the structure–reactivity relationship of functional monomers is essential to gain access to materials with chemical functionality *via* direct polymerisation. Herein, we report how structural modifications of alkyl-substituted  $\epsilon$ -caprolactones affected their reactivity towards the ring-opening of the functional monomer. We observed that the reactivity was strongly influenced by the substituent position, wherein the  $\delta$ -substituted monomer exhibited the fastest polymerisation kinetics. In contrast, a substituent placement in the  $\epsilon$ -position significantly reduced polymerisation time compared to other substituent positions. Moreover, the thermal properties of the resultant functional  $\epsilon$ -polycaprolactones were investigated and showed no significant change in the thermal transitions. This demonstrates that functional caprolactone monomers with sterically demanding functional groups can still undergo direct ring-opening polymerisation and that careful positioning of these functional groups enables control of the rate of polymerisation, a crucial parameter to be considered for the design of new prospective functional monomers and their industrial applications.

Received 13th December 2023,  
Accepted 20th February 2024

DOI: 10.1039/d3py01380d

rsc.li/polymers

## Introduction

Aliphatic polyesters are an attractive and versatile class of polymeric materials that can undergo degradation by hydrolysis, as well as, in some cases, degrade in the environment.<sup>1–3</sup> Their application ranges from commodity thermoplastics to biomaterials for tissue engineering or drug delivery devices.<sup>4–6</sup> In particular, polycaprolactones (PCLs) have been the subject of considerable interest owing to their low toxicity, biocompatibility and biodegradability.<sup>7–9</sup> Synthetically, PCL can be obtained either by step-growth polycondensation of hydroxycarboxylic acids or ring-opening polymerisation (ROP) of lactones.<sup>4</sup> While polycondensation reactions allow the production of a wider range of functional polyesters, they often require long reaction times and high temperatures, resulting in poor control over the molar mass.<sup>4</sup> By contrast, ROP enables the generation of polyesters with good control over polymerisation, predictable

molar mass and narrow dispersities.<sup>10,11</sup> As a consequence, the ROP of lactones constitutes the method of choice for the synthesis of PCL and has been extensively studied using a variety of catalytic systems and initiators.<sup>12–15</sup> However, a major limitation towards the development of new materials results from the lack of readily tuneable side chain functionality, which prevents direct functionalisation to be performed on the polymer backbone. Indeed, the presence of functional groups is highly desirable for the design of new potential monomers as it allows important polymer properties such as crystallinity, biodegradation rate or mechanical properties to be tailored.<sup>16</sup>

Over the past two decades several strategies for the synthesis of functional polycaprolactones have been developed. A common approach is to graft functional groups onto pre-formed polymer chains bearing a reactive pendant group such as azides,<sup>17</sup> alkynes<sup>18</sup> or epoxides.<sup>19</sup> This approach allows the introduction of a variety of functional groups *via e.g.* click chemistry,<sup>20,21</sup> cycloadditions<sup>22</sup> or metathesis reactions.<sup>23</sup> However, these reactions are often limited by functionality, scalability and contamination by catalysts and/or chemicals used to perform the post-polymerisation functionalisation.<sup>4</sup> To overcome these predicaments, the direct polymerisation of

<sup>a</sup>School of Chemistry, University of Birmingham, Edgbaston, Birmingham B15 2TT, UK. E-mail: r.oreilly@bham.ac.uk, a.dove@bham.ac.uk

<sup>b</sup>Infineum UK Ltd, Milton Hill, Abingdon OX13 6BB, UK

† Electronic supplementary information (ESI) available. See DOI: <https://doi.org/10.1039/d3py01380d>



functional monomers offers highly effective and efficient synthesis with greater control over monomer purity, polymer composition and the ability to produce block copolymers without the need of a further modification step.<sup>24,25</sup> Therefore, the direct ROP of monomers containing functional groups is often more desirable to develop more universal polymerisation strategies for *e.g.* industrial applications.

The ROP of functional  $\epsilon$ -caprolactones has been widely studied using simple functional monomers including lactone substituted with halogenides,<sup>26,27</sup> acrylates<sup>28</sup> or terminal olefins.<sup>29</sup> However, the addition of new functional groups, particularly those in close proximity to the active ring-opening centre, can promote steric hindrance and influence the ring-opening polymerisation kinetics. In order to enhance the understanding of substituent effects on monomer polymerisability, Hillmyer and co-workers systematically studied the polymerisation thermodynamics and kinetics of a series of *n*-alkyl-substituted  $\delta$ -valerolactones with a focus on the effect of alkyl substituent sizes and regiochemistry on the polymerisation rate.<sup>30</sup> The authors found that the regiochemistry of a methyl substituent influenced the polymerisation rate. Monomers substituted in  $\alpha$ - and  $\beta$ -position polymerised at a rate comparable to the unsubstituted monomer, whereas a substituent placed in the  $\delta$ -position made the polymerisation an order of magnitude slower.<sup>30</sup> Considering the importance of exploiting novel functional caprolactones, we envisioned that a comparative study of how sterically demanding alkyl substituents influence the ring-opening kinetics would enhance the understanding of the structure–reactivity relationship, a fundamental parameter to be evaluated prior to polymer applications on a larger scale.

Herein, we describe the direct preparation of functional lipophilic polyesters *via* well-controlled ring-opening polymerisation using alkyl-functionalised  $\epsilon$ -caprolactone ( $\epsilon$ CL) monomers. In particular, we sought to investigate the relationship between the substituent position on the  $\epsilon$ CL ring and the reaction rate, by using four different alkyl-functionalised caprolactone isomers:  $\gamma$ C<sub>18</sub>CL, a mixture of two isomers substituted in  $\beta$ - and  $\delta$ -position ( $\beta/\delta$ C<sub>18</sub>CL isomers), and  $\epsilon$ C<sub>18</sub>CL. Moreover, the effect of the alkyl chain position on the thermal properties of the formed polymers was also investigated.

## Experimental

### Materials

Chemicals and solvents, unless otherwise stated, were purchased from Sigma-Aldrich and Fisher Scientific and used without further purification. Deuterated benzene was ordered from Apollo Scientific, degassed by repeated freeze-pump-thawing and then dried under reflux over sodium and benzophenone before storing it under an inert atmosphere of N<sub>2</sub>. Deuterated chloroform was ordered from Apollo Scientific, dried over molecular sieves 3 times and deoxygenated with N<sub>2</sub> before storing it under an inert atmosphere of N<sub>2</sub>. Diphenyl phosphate was dried under reduced pressure at 50 °C for 3

days. 4-Methoxybenzyl alcohol was dried over CaH<sub>2</sub> for 24 h and distilled under reduced pressure before storing it under an inert atmosphere of N<sub>2</sub>. Amberlyst A21 free base was washed repeatedly with methanol and dried under reduced pressure prior to use. The alkyl-substituted monomers,  $\gamma$ C<sub>18</sub>CL,  $\beta/\delta$ C<sub>18</sub>CL isomers and  $\epsilon$ C<sub>18</sub>CL were received from Infineum UK Ltd (Schemes S1–S3†), dissolved in dry CH<sub>2</sub>Cl<sub>2</sub> and dried over CaH<sub>2</sub> for 24 h (and this was repeated 1× with fresh CaH<sub>2</sub>). Excess CaH<sub>2</sub> was removed by cannula filtration and CH<sub>2</sub>Cl<sub>2</sub> was distilled off under reduced pressure before storing the monomers under an inert atmosphere of N<sub>2</sub>.

### General considerations

All polymerisations were performed under an inert nitrogen atmosphere in a glovebox unless otherwise stated. All other chemical manipulations were performed using standard Schlenk-line techniques. <sup>1</sup>H NMR and <sup>13</sup>C NMR spectra were recorded on a Bruker DPX-300, DPX-400 or HD500 spectrometer. Chemical shifts are reported in ppm. Solvent residual signals were used as reference (CDCl<sub>3</sub>, <sup>1</sup>H:  $\delta$  = 7.26 ppm for CHCl<sub>3</sub>, <sup>13</sup>C:  $\delta$  = 77.16 ppm for CDCl<sub>3</sub>; C<sub>6</sub>D<sub>6</sub>, <sup>1</sup>H:  $\delta$  = 7.16 ppm for C<sub>6</sub>D<sub>5</sub>H and <sup>13</sup>C:  $\delta$  = 128.06 ppm for C<sub>6</sub>D<sub>6</sub>). The signals are characterised as s = singlet, d = doublet, t = triplet, q = quartet and m = multiplet. The coupling constant *J* is recorded in Hertz (Hz). Size exclusion chromatography (SEC) measurements were performed on an Agilent 1260 Infinity II Multi-Detector GPC/SEC System fitted with RI, ultraviolet (UV,  $\lambda$  = 309 nm), and viscometer detectors. The polymers were eluted through an Agilent guard column (PLGel 5  $\mu$ M, 50  $\times$  7.5 mm) and two Agilent mixed-C columns (PLGel 5  $\mu$ M, 300  $\times$  7.5 mm) using CHCl<sub>3</sub> (buffered with 0.5% v/v NEt<sub>3</sub>) as the mobile phase (flow rate = 1 mL min<sup>−1</sup>, 40 °C). Number average molar mass (*M*<sub>n</sub>), weight average molar mass (*M*<sub>w</sub>) and dispersities (*D*<sub>M</sub> = *M*<sub>w</sub>/*M*<sub>n</sub>) were determined using Agilent GPC/SEC software (vA.02.01) against a 15-point calibration curve (*M*<sub>p</sub> = 162–3 187 000 g mol<sup>−1</sup>) based on poly(styrene) standards (Easivial PS-M/H, Agilent). Number average molar mass (*M*<sub>n</sub>), weight average molar mass (*M*<sub>w</sub>) are given in g mol<sup>−1</sup>. The thermal characteristics of the polymers were determined using differential scanning calorimetry (DSC) on a STARE DSC3 system from Mettler Toledo and analysed in 40  $\mu$ L aluminium pans from −100–200 °C at a heating rate of 10 °C min<sup>−1</sup> for two heating/cooling cycles or 1 °C min<sup>−1</sup> for one heating/cooling cycle. TGA data was obtained using a Q50 Thermogravimetric Analyzer (TA instruments). Thermograms were recorded under an N<sub>2</sub> atmosphere using a heating rate of 10 °C min<sup>−1</sup>, from 25–500 °C, with an average sample weight of *ca.* 10 mg. Decomposition temperatures were reported as the 5% weight loss temperature (*T*<sub>d</sub> 5%).

### Standard procedure for DPP catalysed polymerisations

Using standard glovebox techniques, a stock solution was prepared containing 4-methoxybenzyl alcohol initiator (55.0 mg, 0.40 mmol) and dry benzene-*d*<sub>6</sub> (500  $\mu$ L). The stock solution (50  $\mu$ L) was added to the appropriate monomer (2 mmol) and catalyst (50.0 mg, 0.20 mmol) in dry benzene-*d*<sub>6</sub> (1.95 mL) to



form a 1 M solution. The solution was then transferred into a vial. Aliquots were taken at allotted time points and quenched by the addition of Amberlyst® A21 free base. After determining the polymer conversion by  $^1\text{H}$  NMR spectroscopy, Amberlyst® was removed *via* filtration through a pipette plugged with cotton wool and the polymer was precipitated into cold MeOH, cooled using liquid nitrogen. Polymers were dried under vacuum.

**For  $\gamma(\text{C}_{18})\text{poly}(\epsilon\text{-caprolactone})$ .**  $^1\text{H}$  NMR (300 MHz,  $\text{CDCl}_3$ , 299 K, ppm):  $\delta$  = 6.96–6.77 (m, 2H,  $\text{CH}_{\text{aromatic}}$ ), 5.04 (s, 2H,  $\text{CH}_2$ ), 4.08 (t,  $J$  = 7.1 Hz, 95H,  $(\text{CO})\text{OCH}_2$ ), 3.81 (s, 3H,  $\text{OCH}_3$ ), 2.28 (t,  $J$  = 7.8 Hz, 103H,  $(\text{CO})\text{OCH}_2$ ), 1.86–1.35 (m, 208H,  $\text{CH}_2$ ), 1.37–1.14 (m, 1806H,  $\text{CH}_2$ ), 0.99–0.63 (m, 155H,  $\text{CH}_3$ ).

$^{13}\text{C}$  NMR (101 MHz,  $\text{CDCl}_3$ , 299 K, ppm):  $\delta$  = 173.9 ( $\text{C}=\text{O}$ ), 62.8 ( $\text{CH}_2\text{O}$ ), 61.0 ( $\text{CH}_2$ ), 34.4 ( $\text{CH}$ ), 33.3 ( $\text{CH}_2$ ), 32.3 ( $\text{CH}_2$ ), 32.08 ( $\text{CH}_2$ ), 31.7 ( $\text{CH}_2$ ), 30.2 ( $\text{CH}_2$ ), 29.9 ( $\text{CH}_2$ ), 29.9 ( $\text{CH}_2$ ), 29.8 ( $\text{CH}_2$ ), 29.5 ( $\text{CH}_2$ ), 28.8 ( $\text{CH}_2$ ), 26.6 ( $\text{CH}_2$ ), 22.8 ( $\text{CH}_2$ ), 14.3 ( $\text{CH}_3$ ).

SEC ( $\text{CHCl}_3$ ):  $M_n$  = 11 350,  $M_w$  = 12 700,  $D_M$  = 1.12.

**For  $\beta/\delta(\text{C}_{18})\text{poly}(\epsilon\text{-caprolactone})$  isomers.**  $^1\text{H}$  NMR (300 MHz,  $\text{CDCl}_3$ , 299 K, ppm):  $\delta$  = 6.88 (d,  $J$  = 8.7 Hz, 2H,  $\text{CH}_{\text{aromatic}}$ ), 5.04 (s, 2H,  $\text{CH}_2$ ), 4.18–3.92 (m, 93H,  $(\text{CO})\text{OCH}_2$ ), 3.80 (s, 3H,  $\text{OCH}_3$ ), 2.43–2.14 (m, 104H,  $(\text{CO})\text{OCH}_2$ ), 1.87 (s, 53H,  $\text{CH}_2$ ), 1.76–1.51 (m, 135H,  $\text{CH}_2$ ), 1.25 (s, 2035H,  $\text{CH}_2$ ), 0.87 (d,  $J$  = 7.0 Hz, 177H,  $\text{CH}_3$ ).

$^{13}\text{C}$  NMR (101 MHz,  $\text{CDCl}_3$ , 299 K, ppm):  $\delta$  = 173.6 ( $\text{C}=\text{O}$ ), 66.9 ( $\text{CH}_2\text{O}$ ), 36.9 ( $\text{CH}$ ), 34.5 ( $\text{CH}_2$ ), 32.0 ( $\text{CH}_2$ ), 31.1 ( $\text{CH}_2$ ), 30.9 ( $\text{CH}_2$ ), 30.0 ( $\text{CH}_2$ ), 29.8 ( $\text{CH}_2$ ), 29.7 ( $\text{CH}_2$ ), 29.7 ( $\text{CH}_2$ ), 29.4 ( $\text{CH}_2$ ), 26.7 ( $\text{CH}_2$ ), 26.6 ( $\text{CH}_2$ ), 22.7 ( $\text{CH}_2$ ), 22.2 ( $\text{CH}_2$ ), 14.2 ( $\text{CH}_3$ ).

SEC ( $\text{CHCl}_3$ ):  $M_n$  = 6350,  $M_w$  = 6900,  $D_M$  = 1.09.

**For  $\epsilon(\text{C}_{18})\text{poly}(\epsilon\text{-caprolactone})$ .**  $^1\text{H}$  NMR (400 MHz,  $\text{CDCl}_3$ , 299 K, ppm):  $\delta$  = 6.81 (d,  $J$  = 8.7 Hz, 2H,  $\text{CH}_{\text{aromatic}}$ ), 4.96 (s, 2H,  $\text{CH}_2$ ), 4.78 (t,  $J$  = 6.2 Hz, 48H,  $(\text{CO})\text{OCH}$ ), 3.73 (s, 3H,  $\text{OCH}_3$ ), 2.19 (t,  $J$  = 7.6 Hz, 104H,  $(\text{CO})\text{OCH}_2$ ), 1.65–1.33 (m, 275H,  $\text{CH}_2$ ), 1.18 (d,  $J$  = 2.4 Hz, 1852H,  $\text{CH}_2$ ), 0.81 (t,  $J$  = 6.7 Hz, 167H,  $\text{CH}_3$ ).  $^{13}\text{C}$  NMR (101 MHz,  $\text{CDCl}_3$ , 299 K, ppm):  $\delta$  = 173.4 ( $\text{C}=\text{O}$ ), 74.0 ( $\text{CHO}$ ), 50.9 ( $\text{CH}_2$ ), 34.5 ( $\text{CH}_2$ ), 34.0 ( $\text{CH}_2$ ), 33.9 ( $\text{CH}_2$ ), 32.0 ( $\text{CH}_2$ ), 29.8 ( $\text{CH}_2$ ), 29.7 ( $\text{CH}_2$ ), 29.7 ( $\text{CH}_2$ ), 29.7 ( $\text{CH}_2$ ), 29.6 ( $\text{CH}_2$ ), 29.6 ( $\text{CH}_2$ ), 29.4 ( $\text{CH}_2$ ), 25.4 ( $\text{CH}_2$ ), 25.0 ( $\text{CH}_2$ ), 22.7 ( $\text{CH}_2$ ), 14.1 ( $\text{CH}_3$ ).

SEC ( $\text{CHCl}_3$ ):  $M_n$  = 10 100,  $M_w$  = 12 500,  $D_M$  = 1.23.

## Results and discussion

### Ring-opening polymerisation of *n*-alkyl-substituted caprolactones

The alkyl-substituted monomers,  $\gamma\text{C}_{18}\text{CL}$ ,  $\epsilon\text{C}_{18}\text{CL}$  and the mixture of the  $\beta$ - and  $\delta\text{C}_{18}\text{CL}$  isomers, were each polymerised under identical conditions using diphenyl phosphate (DPP) (10 mol%) as the catalyst and 4-methoxybenzyl alcohol as the initiator ( $[\text{M}]_0/[\text{I}]_0 = 50$ ) (Scheme 1). DPP enables the ROP of lactones with high control over molar mass regardless of the monomer structure and was therefore chosen as the catalyst for this study.<sup>30,31</sup>



**Scheme 1** General scheme for the ring-opening polymerisation of *n*-alkyl-substituted  $\epsilon$ -caprolactone monomers.

Each polymerisation was monitored independently by  $^1\text{H}$  NMR spectroscopy following the disappearance of  $\text{CH}_2\text{OC}=\text{O}$  monomer resonance ( $\delta$  = 3.7 ppm, Fig. 1) and the appearance of the  $\text{CH}_2\text{OC}=\text{O}$  polymer resonance ( $\delta$  = 4.2 ppm, Fig. 1); as shown for  $\gamma\text{C}_{18}\text{CL}$  in Fig. 1. For this particular monomer, a decrease in the monomer concentration was observed, reaching a monomer conversion of 90% within 2.5 h. In order to study the polymerisation control, aliquots were taken from the individual polymerisations, quenched by the addition of a solid-support base (Amberlyst®) and further analysed by size exclusion chromatography (SEC) and  $^1\text{H}$  NMR spectroscopy.

All studied polymerisations demonstrated a linear increase of molar mass with conversion (Fig. 2), indicating a well-controlled polymerisation. This could be further confirmed by  $^1\text{H}$  NMR spectroscopy of the precipitated polymers, which revealed the characteristic peaks of the PCL backbone with the pendant alkyl moieties and well-defined end-group signals (Fig. S4–S6†). These were used to confirm a degree of polymerisation (DP) close to the targeted DP. SEC analysis further confirmed the well-controlled nature of the polymerisations with dispersities between 1.09 and 1.23. (Table 1 and Fig. S7–



**Fig. 1** (a) ROP of  $\gamma\text{C}_{18}\text{CL}$  using DPP (10 mol%), 4-methoxybenzyl alcohol ( $[\text{M}]_0/[\text{I}]_0 = 50$ ), benzene- $d_6$ . (b) Stacked  $^1\text{H}$  NMR spectra (benzene- $d_6$ , 300 MHz) during ROP of  $\gamma\text{C}_{18}\text{CL}$  showing the  $\text{CH}_2\text{OC}=\text{O}$  monomer resonance between  $\delta$  = 3.37–3.70 ppm and  $\text{CH}_2\text{OC}=\text{O}$  polymer resonance at  $\delta$  = 4.2 ppm.





**Fig. 2** Number-average molar mass ( $M_n$ ) plotted against monomer conversion for the ROP of  $\gamma$ -C<sub>18</sub>CL,  $\epsilon$ -C<sub>18</sub>CL and  $\beta/\delta$ -C<sub>18</sub>CL isomers using DPP (10 mol%) and 4-methoxybenzyl alcohol as initiator ( $[M]_0/[I]_0 = 50$ ). Number-average molar mass ( $M_n$ ) determined by SEC analysis in CHCl<sub>3</sub> (0.5% NEt<sub>3</sub>), calibrated against polystyrene standards.

**Table 1** Ring-opening polymerisation of n-alkyl-substituted caprolactone monomers using DPP (10 mol%)<sup>a</sup>

Monomer	Reaction Time (h)	Monomer Conversion (%) <sup>b</sup>	$M_n$ (kg mol <sup>-1</sup> ) <sup>c</sup>	$M_n$ (kg mol <sup>-1</sup> ) <sup>d</sup>	$D_M^d$
$\gamma$ -C <sub>18</sub> CL	3.4	86	17.5	11.4	1.12
$\beta/\delta$ -C <sub>18</sub> CL (1 : 1 ratio)	4	78	17.1	6.4	1.09
$\epsilon$ -C <sub>18</sub> CL	207	82	17.7	10.1	1.23

<sup>a</sup> DPP (10 mol%) and 4-methoxybenzyl alcohol as initiator ( $[M]_0/[I]_0 = 50$ ) at 25 °C in benzene-*d*<sub>6</sub>. <sup>b</sup> Determined by integrating end-groups using <sup>1</sup>H NMR spectroscopy (benzene-*d*<sub>6</sub>, 298 K). <sup>c</sup> Determined by <sup>1</sup>H NMR spectroscopy (CDCl<sub>3</sub>, 298 K) analysis by integrating end-group signal and CH<sub>2</sub>OC=O polymer resonance ( $\delta = 4.2$  ppm). <sup>d</sup> Determined by SEC analysis in CHCl<sub>3</sub> (0.5% NEt<sub>3</sub>) as eluent and calibrated against polystyrene standards.

S9†) It should be noted that  $\epsilon$ -C<sub>18</sub>PCL showed a small shoulder at higher molar mass, which can be explained by the presence of transesterification side reactions occurring at high monomer conversions (Fig. S9†). Overall, these results confirm that ROP is a method that enables the synthesis of a range of functional polycaprolactones while maintaining control over polymerisation parameters such as molar mass and dispersity.

### Kinetic resolution of the $\beta$ - and $\delta$ -C<sub>18</sub>CL isomers

Notably, while the increase of  $M_n$  with conversion showed a linear behaviour in all cases, the kinetic plots showed first order behaviour only for the pure monomers  $\gamma$ -C<sub>18</sub>CL and  $\epsilon$ -C<sub>18</sub>CL. Not surprisingly, the mixture of the  $\beta$ - and  $\delta$ -C<sub>18</sub>CL isomers displayed a non-linear relationship of the semilogarithmic plot, giving first indication that both monomers polymerise at different rates (Fig. 3b). <sup>1</sup>H NMR spectroscopic analysis in benzene-*d*<sub>6</sub> did not show any resolution between the CH<sub>2</sub>OC=O polymer resonance ( $\delta = 4.2$  ppm) of the  $\beta$ - or  $\delta$ -substituted C<sub>18</sub>PCL. Therefore, to assess the progression of

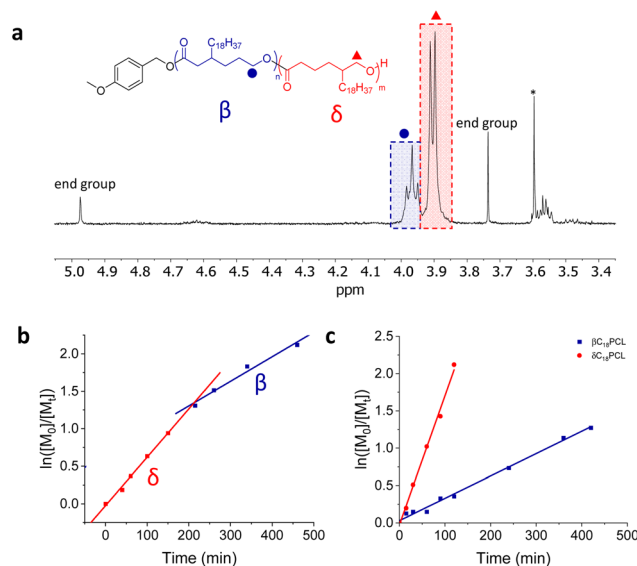


**Fig. 3** (a) <sup>1</sup>H NMR spectrum (CDCl<sub>3</sub>, 400 MHz) of  $\beta$  and  $\delta$ -C<sub>18</sub>PCL. \* = MeOH. (b) Semi-logarithmic kinetic plot time for the ROP of  $\beta/\delta$ -C<sub>18</sub>CL isomers. (c) Resolved semi-logarithmic kinetic plot for the ROP of  $\beta/\delta$ -C<sub>18</sub>CL isomers.  $[M]_0 = 0.5$  M (calculated by NMR spectroscopy based on a starting ratio of  $\beta$  isomer :  $\delta$  isomer = 1 : 1).

the polymerisation of the two isomers, individual kinetic points were taken at allotted times, precipitated into methanol and re-dissolved in chloroform-*d*. The ratio of the  $\beta$ - to  $\delta$ -isomers was evaluated by comparing the CH<sub>2</sub>OC=O integrals ( $\delta = 4.0$  and 3.9 ppm, respectively), which showed distinct splitting patterns (Tables 2 and S1†). The CH<sub>2</sub>OC=O resonance splitting into a doublet can be assigned to  $\delta$ -C<sub>18</sub>PCL, whereas the triplet corresponds to the  $\beta$ -C<sub>18</sub>PCL isomer (Fig. 3a). The linearity of the resolved semi-logarithmic plot indicates first order kinetics in all cases with the  $\delta$ -substituted C<sub>18</sub>PCL displaying the fastest polymerisation rate (Fig. 3c). Using this kinetic resolution experiment allows the comparison of the polymerisation rate of all 4 alkyl-substituted monomers at fixed catalyst and initiator concentration (Fig. 4). Not surprisingly, the rate of polymerisation is strongly dependent on the position of the substituent. While  $\delta$ - and  $\gamma$ -substituted C<sub>18</sub>εCL displayed the fastest kinetics, with monomer conversion of around 85% reached within 3 h, the  $\beta$ -position seemed to have a greater impact on the ROP kinetics, possibly owing to an increased steric hindrance. In contrast to these findings, when the C<sub>18</sub>-substituent was placed in the  $\epsilon$ -position, a substantially reduced rate of polymerisation was observed such that a monomer conversion of only 80% could be obtained within 9 days. We propose that the significantly slower kinetics are the result of high levels of steric hindrance around the carbonyl functionality (kinetics:  $\delta$ -C<sub>18</sub> >  $\gamma$ -C<sub>18</sub> >  $\beta$ -C<sub>18</sub> >>  $\epsilon$ -C<sub>18</sub>). These results are similar to those observed by Hillmyer and co-workers, where a series of alkyl-substituted  $\delta$ -valerolactones were investigated. Among the methyl-substituted lactones, the  $\gamma$ -substituted derivative exhibited the fastest polymerisation rate, whereas the  $\delta$ -substituted  $\delta$ -valerolactone was reported to





**Table 2** Kinetic resolution of the ROP of the constitutional isomers  $\beta/\delta\text{C}_{18}\text{CL}^a$ 

Time (min)	Total conversion <sup>b</sup> (%)	$\beta\text{-C}_{18}\text{PCL}$ isomer : $\delta\text{-C}_{18}\text{PCL}$ isomer <sup>c</sup>	Resolved conversion ( $\beta$ isomer) <sup>d</sup> (%)	Resolved conversion ( $\delta$ isomer) <sup>d</sup> (%)
15	15	1 : 1.6	12	18
30	27	1 : 3	14	40
60	39	1 : 4.5	14	64
90	53	1 : 2.7	28	76
120	60	1 : 2.9	30	88
240	78	1 : 1.9	52	—
360	85	1 : 1.2	68	—
420	92	1 : 1.1	72	—

<sup>a</sup> ROP of  $\beta/\delta(\text{C}_{18})\text{CL}$  isomers using DPP and 4-methoxybenzyl alcohol as initiator ( $[\text{M}]_0/[\text{I}]_0 = 50$ ).  $[\text{M}] = 1 \text{ M}$ . <sup>b</sup> Determined by  $^1\text{H}$  NMR spectroscopy in benzene- $d_6$ . <sup>c</sup> Determined by  $^1\text{H}$  NMR spectroscopy in  $\text{CDCl}_3$  by integration of  $\text{CH}_2\text{OC}=\text{O}$  integrals at  $\delta = 4.0$  and  $3.9 \text{ ppm}$ . <sup>d</sup> Calculated from isomer ratios obtained by  $^1\text{H}$  NMR spectroscopy based on a total monomer concentration of  $1 \text{ M}$  and a starting ratio of  $\beta$  isomer :  $\delta$  isomer =  $1 : 1$ .



**Fig. 4** Semi-logarithmic kinetic plot for ROP of  $\epsilon\text{C}_{18}\text{CL}$ ,  $\gamma\text{C}_{18}\text{CL}$  and  $\beta/\delta\text{C}_{18}\text{CL}$  isomers using DPP (10 mol%) and 4-methoxybenzyl alcohol as initiator ( $[\text{M}]_0/[\text{I}]_0 = 50$ ).  $\ln([\text{M}]_0/[\text{M}]_t)$  was determined by  $^1\text{H}$  NMR spectroscopy.

have the slowest polymerisation rate, likely as the result of the relatively low reactivity of the propagating secondary alcohol.<sup>30</sup> Nevertheless, the sluggish polymerisation rate of  $\epsilon\text{C}_{18}\text{CL}$  could be further improved by increasing the temperature from 25 to 50 °C or by changing the catalyst from DPP to  $\text{Mg}(\text{BHT})_2(\text{THF})_2$  (Fig. S10†).

### Thermal properties of the $\text{C}_{18}$ -substituted PCLs

In order to probe how the substituent position affects the thermal properties of the obtained polymers, differential scanning calorimetry (DSC) analysis was performed on  $\gamma\text{C}_{18}\text{PCL}$ ,  $\epsilon\text{C}_{18}\text{PCL}$  and  $\beta/\delta\text{C}_{18}\text{PCL}$  isomers with a degree of polymerisation (DP) of 50 ( $[\text{M}]_0/[\text{I}]_0 = 50$ ) (Fig. 5 and S11†). All three polymers exhibited a sharp first-order melting and crystallisation transition ( $T_m$  and  $T_c$ ). The glass transition temperature ( $T_g$ ) could not be observed, possibly owing to it being masked by the intensity of the  $T_m$  and  $T_c$  transition. The observed crystallinity is likely the result of a cooperative organisation of the

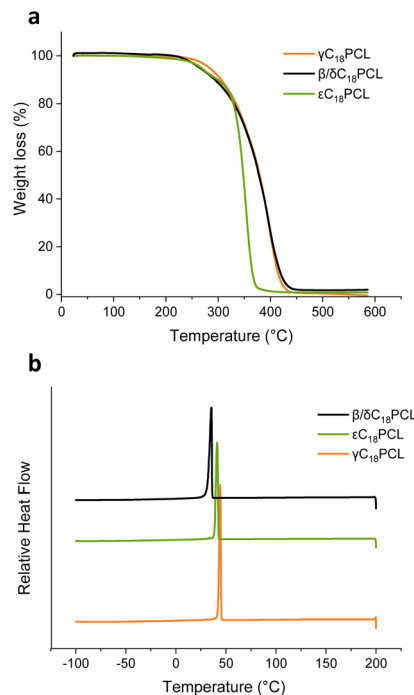


**Fig. 5** (a) Thermogravimetric analysis (TGA) of  $\gamma\text{C}_{18}\text{PCL}$ ,  $\epsilon\text{C}_{18}\text{PCL}$  and  $\beta/\delta\text{C}_{18}\text{PCL}$  isomers. Analytical data of the analysed polymers is summarised in Table 1. (b) Differential scanning calorimetry (DSC) for 2<sup>nd</sup> cooling cycle (200 to  $-100 \text{ }^\circ\text{C}$ ,  $10 \text{ }^\circ\text{C min}^{-1}$ ) showing crystallisation and melting temperature of the polymers.

pendant  $\text{C}_{18}$  alkyl chains, which has been previously reported to enhance the overall order in the polymers.<sup>32,33</sup> However, when comparing the three different constitutional isomers only slight differences in the  $T_m$  and  $T_c$  could be observed with  $\gamma\text{C}_{18}\text{PCL}$  displaying the highest  $T_m$  of 49 °C while  $\beta/\delta\text{C}_{18}\text{PCL}$  isomers displayed the lowest  $T_m$  of 42 °C (Table 3). The lower  $T_m$  of the  $\beta/\delta\text{C}_{18}\text{PCL}$  isomers is likely the result of the presence of two substituent sides in the polymers, which thereby disrupt the packing of the  $\text{C}_{18}$ -alkyl chains in the polymer. Thermogravimetric analysis (TGA) revealed a weight loss of 5% at 280 °C for  $\gamma\text{C}_{18}\text{PCL}$  and at around 260 °C for both  $\epsilon\text{C}_{18}\text{PCL}$  and  $\beta/\delta\text{C}_{18}\text{PCL}$  isomers, although  $\epsilon\text{C}_{18}\text{PCL}$  isomers showed a



**Table 3** Differential scanning calorimetry data and thermogravimetric data of  $\gamma$ C<sub>18</sub>PCL,  $\epsilon$ C<sub>18</sub>PCL and  $\beta/\delta$ C<sub>18</sub>PCL isomers

Polymer	$T_m^a$ (°C)	$T_c^a$ (°C)	$\Delta H_m^b$ (J g <sup>-1</sup> )	$T_d^c$ 5% (°C)
$\gamma$ C <sub>18</sub> PCL	49	44	-60.2	280
$\beta/\delta$ C <sub>18</sub> PCL isomers	42	35	-35.8	262
$\epsilon$ C <sub>18</sub> PCL	47	41	-32.6	265

<sup>a</sup>  $T_m$  and  $T_c$  were determined by differential scanning calorimetry and were obtained from the 2<sup>nd</sup> heating cycle and cooling cycle, respectively. <sup>b</sup> Total enthalpy of melting ( $\Delta H_m$ ) was calculated by integration of the first-order endothermic transition. <sup>c</sup> Determined by TGA at 5% weight loss.

much sharper weight loss compared  $\beta/\delta$ C<sub>18</sub>PCL (Fig. 5a). Nevertheless, all three polymers exhibit thermal stability below 250 °C, making them a suitable material for a range of industrial applications. Overall, it could be demonstrated that the position of the alkyl chain on the PCL backbone has only minor effects on the thermal properties of the resultant polymers. This demonstrates that the discrete substituents play a major role in polymerisation kinetics, but only have minor effect on the resulting thermal properties.

## Conclusions

We report the well-controlled ring-opening polymerisation of 4 alkyl-substituted  $\epsilon$ -caprolactone monomers. All 4 monomers could be polymerised using the commercially available organo-catalyst DPP to obtain lipophilic polyesters. Although the synthesis of all functional polyesters could be achieved with good control over molar mass and dispersity, the polymerisation rate was strongly dependent on the substituent placement. While the substituents in  $\gamma$ - and  $\delta$ -position had only a minor effect on the overall polymerisation time, with 85% conversion reached in 3 h, the substituent placed in  $\beta$ -position increased polymerisation time to 7 h owing to increasing steric hindrance around the active carbonyl centre. Using identical polymerisation conditions, the  $\epsilon$ -caprolactone monomer with a  $\epsilon$ C<sub>18</sub>-substituent further increased the polymerisation time drastically to 9 days. However, analysis of the thermal properties by DSC and TGA revealed that the substituent position in the resulting functional polyester has only minor impact on properties such as crystallisation and degradation temperature. Overall, this shows that by changing the position of the C<sub>18</sub>-alkyl substituent the relative polymerisation rates can be significantly changed without impacting the thermal properties of the functional polyesters. This highlights how simple substituent placement can be utilised to favour the kinetics of different monomer systems. These fundamental studies are essential to understand synthetic limitations for the design and development of new functional monomers with tailored property profiles and can be utilised to establish guidelines for the design of future materials.

## Conflicts of interest

There are no conflicts to declare.

## Acknowledgements

The authors would like to acknowledge Infineum UK Ltd for funding and delivery of the monomers.

## References

- 1 M. A. Hillmyer and W. B. Tolman, *Acc. Chem. Res.*, 2014, **47**, 2390–2396.
- 2 H. R. Kricheldorf, *Chemosphere*, 2001, **43**, 49–54.
- 3 A. G. A. Coombes, S. C. Rizzi, M. Williamson, J. E. Barralet, S. Downes and W. A. Wallace, *Biomaterials*, 2004, **25**, 315–325.
- 4 C. Jérôme and P. Lecomte, *Adv. Drug Delivery Rev.*, 2008, **60**, 1056–1076.
- 5 O. Coulembier, P. Degée, J. L. Hedrick and P. Dubois, *Prog. Polym. Sci.*, 2006, **31**, 723–747.
- 6 T. K. Dash and V. B. Konkimalla, *J. Controlled Release*, 2012, **158**, 15–33.
- 7 R. J. Pounder and A. P. Dove, *Polym. Chem.*, 2010, **1**, 260–271.
- 8 R. A. Gross and B. Kalra, *Science*, 2002, **297**, 803–807.
- 9 P. Joshi and G. Madras, *Polym. Degrad. Stab.*, 2008, **93**, 1901–1908.
- 10 M. J. Stanford and A. P. Dove, *Chem. Soc. Rev.*, 2010, **39**, 486–494.
- 11 N. E. Kamber, W. Jeong, R. M. Waymouth, R. C. Pratt, B. G. G. Lohmeijer and J. L. Hedrick, *Chem. Rev.*, 2007, **107**, 5813–5840.
- 12 B. G. G. Lohmeijer, R. C. Pratt, F. Leibfarth, J. W. Logan, D. A. Long, A. P. Dove, F. Nederberg, J. Choi, C. Wade, R. M. Waymouth and J. L. Hedrick, *Macromolecules*, 2006, **39**, 8574–8583.
- 13 R. C. Pratt, B. G. G. Lohmeijer, D. A. Long, R. M. Waymouth and J. L. Hedrick, *J. Am. Chem. Soc.*, 2006, **128**, 4556–4557.
- 14 E. Martin, P. Dubois and R. Jérôme, *Macromolecules*, 2003, **36**, 7094–7099.
- 15 A. Kowalski, J. Libiszowski, T. Biela, M. Cypriak, A. Duda and S. Penczek, *Macromolecules*, 2005, **38**, 8170–8176.
- 16 M. Trollsås, V. Y. Lee, D. Mecerreyes, P. Löwenhielm, M. Möller, R. D. Miller and J. L. Hedrick, *Macromolecules*, 2000, **33**, 4619–4627.
- 17 L. Ciani, S. Bortolussi, I. Postuma, L. Cansolino, C. Ferrari, L. Panza, S. Altieri and S. Ristori, *Int. J. Pharm.*, 2013, **458**, 340–346.
- 18 X. Lou, C. Detrembleur, P. Lecomte and R. Jérôme, *Macromolecules*, 2001, **34**, 5806–5811.
- 19 D. Tian, P. Dubois, C. Grandfils and R. Jérôme, *Macromolecules*, 1997, **30**, 406–409.



- 20 J. Xu, F. Prifti and J. Song, *Macromolecules*, 2011, **44**, 2660–2667.
- 21 S. Tempelaar, I. A. Barker, V. X. Truong, D. J. Hall, L. Mespouille, P. Dubois and A. P. Dove, *Polym. Chem.*, 2013, **4**, 174–183.
- 22 R. Riva, S. Schmeits, C. Jérôme, R. Jérôme and P. Lecomte, *Macromolecules*, 2007, **40**, 796–803.
- 23 R. H. Grubbs, *Tetrahedron*, 2004, **60**, 7117–7140.
- 24 H. Seyednejad, A. H. Ghassemi, C. F. van Nostrum, T. Vermonden and W. E. Hennink, *J. Controlled Release*, 2011, **152**, 168–176.
- 25 J. Hao, P. Kos, K. Zhou, J. B. Miller, L. Xue, Y. Yan, H. Xiong, S. Elkassih and D. J. Siegwart, *J. Am. Chem. Soc.*, 2015, **137**, 9206–9209.
- 26 S. Gautier, V. D'Aloia, O. Halleux, M. Mazza, P. Lecomte and R. Jérôme, *J. Biomater. Sci., Polym. Ed.*, 2003, **14**, 63–85.
- 27 M. Su, H. Huang, X. Ma, Q. Wang and Z. Su, *Macromol. Rapid Commun.*, 2013, **34**, 1067–1071.
- 28 D. Mecerreyes, J. Humes, R. D. Miller, J. L. Hedrick, C. Detrembleur, P. Lecomte, R. Jérôme and J. San Roman, *Macromol. Rapid Commun.*, 2000, **21**, 779–784.
- 29 A. Chen, J. Xu, W. Chiang and C. L. L. Chai, *Tetrahedron*, 2010, **66**, 1489–1495.
- 30 D. K. Schneiderman and M. A. Hillmyer, *Macromolecules*, 2016, **49**, 2419–2428.
- 31 P. V. Persson, J. Schröder, K. Wickholm, E. Hedenström and T. Iversen, *Macromolecules*, 2004, **37**, 5889–5893.
- 32 S. Mete, K. G. Goswami, E. Ksendzov, S. V. Kostjuk and P. De, *Polym. Chem.*, 2019, **10**, 6588–6599.
- 33 S. Zhou, Y. Zhao, Y. Cai, Y. Zhou, D. Wang, C. C. Han and D. Xu, *Polymer*, 2004, **45**, 6261–6268.

